

Local Versus Global Concepts in Hydrodynamic Stability Theory

Olivier Dauchot, Paul Manneville

▶ **To cite this version:**

Olivier Dauchot, Paul Manneville. Local Versus Global Concepts in Hydrodynamic Stability Theory. Journal de Physique II, 1997, 7 (2), pp.371-389. 10.1051/jp2:1997131 . jpa-00248449

HAL Id: jpa-00248449
https://hal.science/jpa-00248449

Submitted on 4 Feb 2008

HAL is a multi-disciplinary open access archive for the deposit and dissemination of scientific research documents, whether they are published or not. The documents may come from teaching and research institutions in France or abroad, or from public or private research centers.

L'archive ouverte pluridisciplinaire **HAL**, est destinée au dépôt et à la diffusion de documents scientifiques de niveau recherche, publiés ou non, émanant des établissements d'enseignement et de recherche français ou étrangers, des laboratoires publics ou privés.

J. Phys. II France 7 (1997) 371–389 FEBRUARY 1997, PAGE 371

Local *Versus* Global Concepts in Hydrodynamic Stability Theory

Olivier Dauchot ([1]) and Paul Manneville ([1,2,*])

([1]) Service de Physique de l'État Condensé, Centre d'Étude de Saclay,
91191 Gif-sur-Yvette, France
([2]) Laboratoire d'Hydrodynamique, École Polytechnique, 91128 Palaiseau, France

(Received 25 July 1996, received in final form 3 October 1996, accepted 25 October 1996)

PACS.47.20.-k – Hydrodynamic stability
PACS.05.45.+b – Theory and models of chaotic systems

Abstract. — Linear and nonlinear issues in the problem of the subcritical transition to turbulence are examined on the basis of a full phase-space analysis of a simplified model that mimics hydrodynamics governed by the Navier-Stokes equations. The simplicity of the model, which involves only two variables and displays both non-normal linear terms and energy conserving nonlinear terms, allows us to perform a complete study. This study strongly suggests to take with care conclusions extrapolated from "local" arguments deriving from linear stability theory, since actual stability boundaries can be decided only from the knowledge of the relevant attraction basins, which is "global" in essence.

1. Introduction

In spite of more than a century of theoretical and experimental efforts, the transition to turbulence in some hydrodynamical flows of current interest is still far from being fully understood. This is so mainly because the most useful tools that can be used remain based on linear and weakly nonlinear concepts. As a matter of fact, much progress has been made for instabilities where the basic state becomes unstable with respect to a new solution that branches off continuously so that the bifurcated state remains within reach of a weakly nonlinear perturbation theory. Classical examples are Rayleigh-Bénard cells in thermal convection and Taylor vortices in the Couette flow between differentially rotating cylinders. The cleanest case is then when subsequent instabilities organize themselves in a cascade where each step can be treated similarly, leading to a Landau-Ruelle-Takens type of picture [1, 2]. Unfortunately, other flows of comparable interest behave more wildly and weakly nonlinear analysis tells us very little, or nothing at all, about their transition to turbulence. Indeed, when the bifurcated state is not close to the basic state perturbation expansions may not converge, which leaves the door open to a direct transition to turbulence [1]. This is even the only possible scenario when the flow is known to remain stable against all infinitesimal perturbations: new relevant solutions then appear generically "from nothing" making a thorough understanding of the transition more delicate.

In this context, the plane Couette flow and the Poiseuille pipe flow, both in the latter class of systems, are of special concern. In practice the natural transition (*i.e.*, from irregularities of the

(*) Author for correspondence (e-mail: pops@ladhyx.polytechnique.fr)

© Les Éditions de Physique 1997

basic flow and without any kind of forcing) hardly leads to reproducible results and it turns out preferable to trigger the transition by generating turbulent spots, as done earlier for the plane Poiseuille flow or the Blasius boundary layer [3,4]. Results in this vein have been obtained only recently, either by direct numerical simulations of the Navier-Stokes (NS) equations in the plane Couette flow case [5] or in the laboratory. In particular, a critical perturbation amplitude below which the flow remains stable was shown to exist first in the plane Couette flow case [6] and later in the Poiseuille pipe flow case [7]. At about the same time, special finite amplitude solutions of the NS equations have been obtained by different contorted ways [8–10]. Simultaneously, a theoretical interpretation of the origin of the nonlinear instability has been put forward in terms of a "bypass mechanism" [11] resting on the transient linear amplification of the kinetic energy contained in the perturbations by a non-normal linear stability operator [12]. In this paper, we intend to clarify some of the issues by setting the problem in the framework of dynamical systems and studying a simple model that displays such relevant features as energy conservation by the nonlinearities or a non-normal linearized dynamics. Before presenting the model and analyzing its phase-space structure in Section 3 we make some general preliminary remarks about the different concepts of stability in Section 2. Section 4 is devoted to a discussion of the problem of transient energy growth within our model and somewhat beyond. Section 5 deals with the determination of nonlinear instability thresholds in case of a subcritical transition to turbulence under natural conditions or by triggering, taking advantage of the phase-space analysis in Section 3, and discusses some consequences for experiments. Our conclusions are summarized in Section 6.

2. Local and Global Stability, Super- and Sub-Criticality, and the Energy

At this stage, let us situate the problem of the transition to turbulence in a sufficiently general framework and first recall that the stability of a given basic state of a flow controlled by some parameter r (usually the Reynolds number) is understood as its ability to recover from perturbations. Generally speaking stability properties depend on r and, assuming that r increases with the distance to the rest state, one defines first a *global stability threshold* r_g by the property that, for $r < r_g$, perturbations of arbitrary shapes and "amplitudes" all decay asymptotically as time tends to infinity: the flow returns to the basic state which is therefore *unconditionally stable*. On the other hand, a threshold of *unconditional instability*, r_ℓ, can be obtained from linear stability analysis. It is characterized by the fact that for $r > r_\ell$ there exists at least one (infinitesimal) perturbation against which the basic state is unstable. Clearly we must have $r_g \leq r_\ell$ but, whereas r_ℓ can be derived from a definite strategy, r_g is not easy to obtain since all possible perturbations have to be tested for, and not only infinitesimal ones whose initial dynamics are governed by a linear operator.

To fill the gap between r_g and r_ℓ one then usually tries to determine the possible solutions in vicinity of r_ℓ by means of one or another variant of expansions in powers $r - r_\ell$. This leads to the concepts of *supercritical* and *subcritical* bifurcations. Indeed, two situations may occur generically: either the new solutions appear beyond the critical point and the system bifurcates continuously toward a stable state (supercritical case, Fig. 1a) or the new solutions already exist before the critical value is reached (subcritical case, Fig. 1b). In the latter case they are unstable and nothing stable branches off the linearly unstable solution ([1]). The quantity A in ordinate of these figures, which is just the amplitude of the most unstable eigenmode of the linear stability problem, can be obtained by an expansion at lowest non-trivial order.

([1]) For simplicity, we omit the case of a *transcritical* bifurcation which corresponds to an exchange of stability between two solutions.

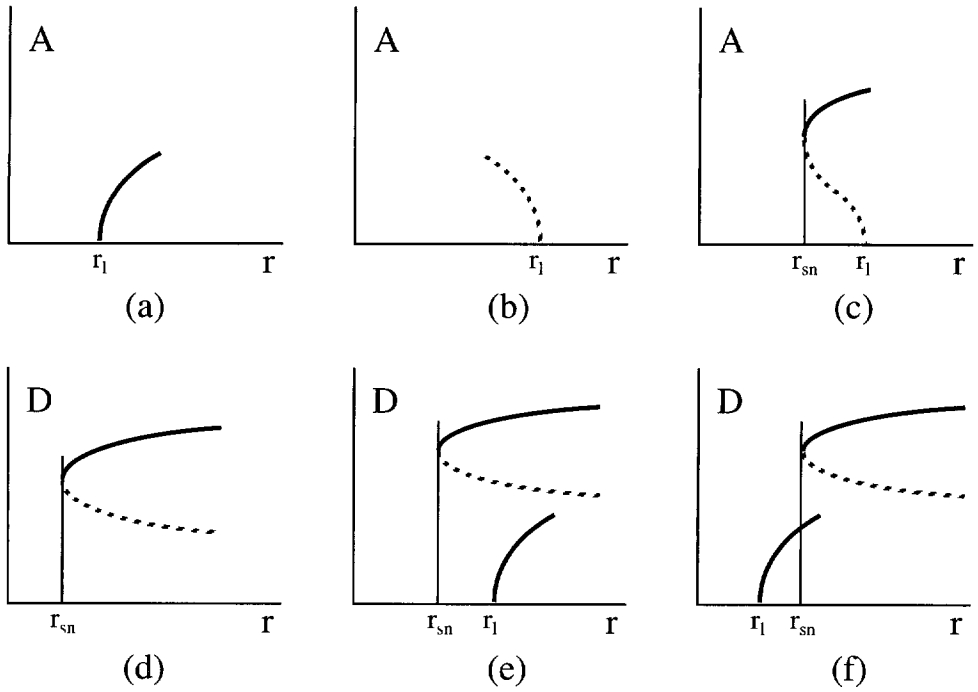


Fig. 1. — Bifurcation diagram in different cases: (a) locally supercritical; (b) locally subcritical (at lowest order); (c) saddle-node arising from locally subcritical (including higher orders); (d) saddle-node from a general standpoint; (e) globally subcritical; (f) globally supercritical. In these figures full lines represent stable states and dashed lines unstable states. A is the amplitude of the bifurcated state. D represents the distance to the basic state when no well-defined mode can be identified, *e.g.*, when the bifurcated state is turbulent (see text).

Of course in the subcritical case the system can find another stable solution, but only at finite distance from the initial state and this new solution usually "disappears" through a *saddle-node bifurcation* at some value $r_{\rm sn}$ of the control parameter. Accordingly, in the range $[r_{\rm sn}, r_\ell]$ two linearly stable solutions coexist, the old and the new (Fig. 1c). In principle, the bifurcated solution can still be obtained by pushing the perturbation expansion at higher orders.

When the basic state is linearly stable for all r, the situation is likely to be as in Figure 1d. The quantity D in ordinate is now just some convenient measure of the "distance" to the basic state but the drawing suggests that the new solutions appear through a saddle-node bifurcation as in Figure 1c. Other cases are also possible, such as that in Figures 1e or 1f, where the basic state bifurcates supercritically at r_ℓ but experiences instability with respect to finite amplitude perturbations beyond some specific threshold. Cases (d) and (e) or (f) clearly call for an extension of the strict meaning of super/sub-criticality that should be reserved for cases (a) and (b). To put things more clearly, one should call cases (a) and (b) "locally super/subcritical" to emphasize the fact that the search for a bifurcated solution (stable or unstable) is performed in the neighborhood of the basic state only. By contrast, the situation displayed in cases (d) or (e) is characterized by the absence of non-trivial solution in the immediate vicinity of the basic state for values of the control parameter close enough to the linear threshold. Accordingly, this search has to be performed in the full phase space, hence the term "global." So, the system can be said "globally subcritical" as soon as an attractor

coexists with the stable basic state; otherwise it is "globally supercritical." Subfigure 1e thus displays the case of a globally subcritical system where the basic state experiences a locally supercritical bifurcation, whereas subfigure 1f represents a globally supercritical system ([2]).

By contrast with notations in Figures 1a–c, the ordinate in Figures 1d–f was labeled D to convey the idea that the "distance" from the basic state could no longer be measured using the amplitude A of a specific mode in the system, understood as the "order parameter" of the bifurcation. To be an appropriate distance, D just needs to be zero when the observed state is indistinguishable from the basic state and strictly positive otherwise. But supplementary properties would clearly be appreciated, and especially a simple physical interpretation. In this respect, the simplest, *a priori* meaningful, quantity is the "energy" $\mathcal{E}$ contained in the perturbation, formally defined as half the square of the Euclidian norm of the difference between the perturbed solution and the basic state. In our hydrodynamic context, this energy is thus nothing but the kinetic energy (per unit mass) contained in the perturbation $\mathbf{v}' = \mathbf{v} - \mathbf{v}_0$, where $\mathbf{v}_0$ is the basic flow and $\mathbf{v}$ the observed solution:

$$\mathcal{E} = \int_{\mathcal{D}} \frac{1}{2} (\mathbf{v}')^2 \, \mathrm{d}^3\mathbf{r} \,, \tag{1}$$

$\mathcal{D}$ being the domain in physical space where the flow develops.

Working with $\mathcal{E}$ is the essence of the *energy method* ([3]) in its simplest form [13]. The stability of the basic state can then be discussed from the evolution of $\mathcal{E}$ and a threshold r_{m} can be defined by the condition that for $r < r_{\mathrm{m}}$ the energy contained in *any* perturbation decays initially. This condition implies that it decays all the time, hence the name of *monotonous stability* threshold (and the subscript "m") for r_{m}. Thresholds r_{g} and r_{m} relate to the behavior of arbitrary perturbations to the basic flow in two different limits, "$t \to \infty$" and "$t \sim 0$" respectively, so that monotonous stability implies global stability but not the converse, *i.e.*, $r_{\mathrm{m}} \leq r_{\mathrm{g}}$. Indeed, while the perturbation must eventually relax if the system is globally stable, nothing forbids its energy to grow initially. All what can be said from this general, so far unspecific, standpoint is summarized in Figure 2 [13, 14].

In hydrodynamics, it turns out that the Navier-Stokes nonlinearity conserves ([4]) energy $\mathcal{E}$ defined by (1) so that r_{m} can be computed from the linear stability problem. Let us denote the corresponding operator by L_r. Implicit in expression (1) is the definition of a canonical scalar product that may serve us to determine the adjoint $L_r^\dagger$ of L_r. When L_r is normal with respect to this scalar product, *i.e.*, $L_r^\dagger$ and L_r commute with each other, the linear instability threshold r_ℓ and the monotonous stability threshold r_{m} coincide ($r_{\mathrm{m}} = r_\ell$) and, since $r_{\mathrm{m}} \leq r_{\mathrm{g}}$ and $r_{\mathrm{g}} \leq r_\ell$, one has $r_{\mathrm{g}} = r_\ell$ so that the (primary) bifurcation is globally supercritical [15]. When L_r is not normal for this scalar product, which is the general case, nothing more can be said on the basis of this "classical" energy and one is left with the inequalities $r_{\mathrm{m}} \leq r_{\mathrm{g}} \leq r_\ell$. However the conditional stability of the basic state can still be discussed in terms of a different, "exotic", energy $\tilde{\mathcal{E}}$ defined as a positive definite quadratic form encoding an appropriately defined scalar product. While $\tilde{\mathcal{E}}$ starts by increasing for some set of (even infinitesimal) initial perturbations,

([2]) Note however that the distant solution branch bears, in general, no relation with the instability mechanism that governs the local bifurcation. The fact that the threshold associated to the distant branch is below or above the linear threshold is thus likely to be a matter of circumstance. The question is then rather whether the distant branch may be "dangerous" with respect to the basic state. Conclusions can be slightly refined in the case of energy-preserving nonlinearities to be examined later.

([3]) More sophisticated approaches would involve appropriate generalized energies known as Lyapunov functionals.

([4]) This is true provided that the perturbation fulfills periodic or homogeneous boundary conditions.

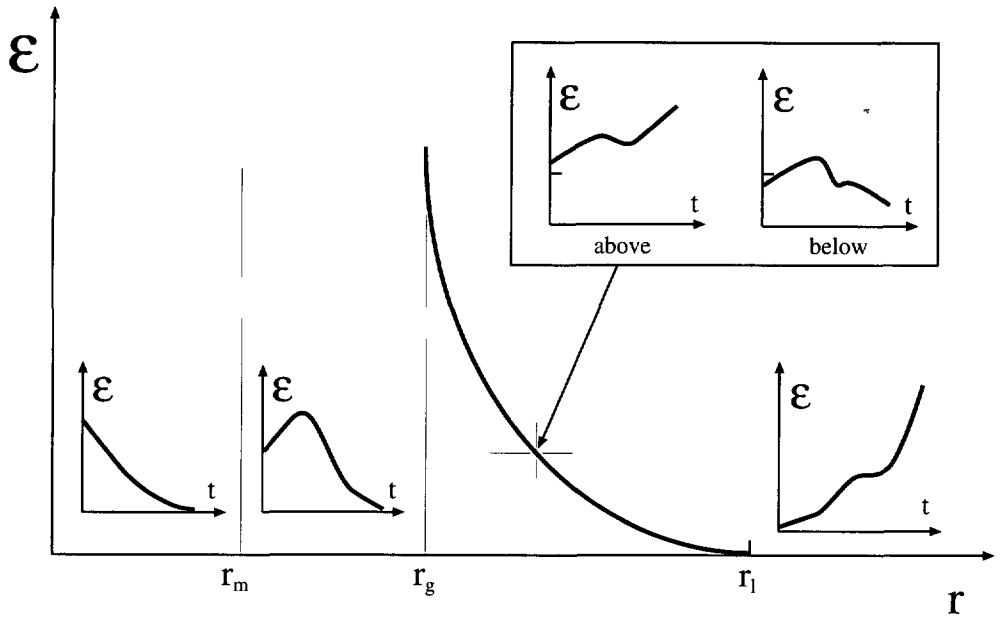


Fig. 2. — The asymptotic behavior of perturbations to the basic state as a function of their initial (classical) energy $\mathcal{E}_0$ and of the value of the control parameter r leads to the definition of thresholds for monotonous stability r_m, global stability r_g, and linear instability r_ℓ.

quantity $\tilde{\mathcal{E}}$ — though no longer conserved by nonlinear terms — always decreases provided it is initially sufficiently small, which is another way to express that the basic state is still linearly stable (see later Fig. 7).

The possibility of transient growth of the classical energy when the linear stability operator is non-normal has been used to discuss the transition to turbulence in globally subcritical cases [16]. The argument was that if the departure from normality is large, small perturbations can be amplified up to a stage where nonlinear interactions trigger a non-trivial response. This appealing approach has been criticized recently, partly on the basis of the fact that the models used to demonstrate the phenomenon were of limited hydrodynamical relevance owing to an insufficient account of the feedback between the basic flow and the perturbation, leading to an overestimation of the role of non-normality [17]. In this paper, our aim is also to question this approach, but from a perhaps even more conceptual standpoint of phase-space analysis of dynamical systems. In this framework, stability properties are analyzed in terms of attractors. For example, a time-independent basic state is a fixed point and, clearly, global stability ($r < r_g$) means that the attraction basin spans the full space of accessible states. By contrast, if the basic state is linearly unstable ($r > r_\ell$) its attraction basin shrinks to nothing. In the range $r_g \leq r \leq r_\ell$, the attraction basin of the basic state is finite and stability is essentially a conditional concept that requires knowledge of the structure of the full phase space.

In the general case, local stability properties derive from the *tangent* dynamics accounting for the behavior of the system in the immediate vicinity of the basic state, which is faithful as long as the nonlinearities are truly negligible. On the other hand, global stability of the basic state can be decided only after trajectories starting everywhere in the phase space have been studied and the *separatrices* delineating the attraction basins have been determined, which is a fully nonlinear highly non-trivial task outside the possibilities of a linearized analysis around

the basic state. One of the aims of this paper is to illustrate this approach in terms of dynamical systems using a model containing some features of the problem of the subcritical transition to turbulence, but sufficiently simplified to be solvable by hand. In light of this study we shall argue that this transition cannot be approached by extrapolation of linear properties in the nonlinear domain and further discuss potential risks of misinterpretation of current experimental procedures to trigger the transition.

3. The Model and its Phase Portrait

To serve our illustrative purpose the chosen model should be both simple and non-trivial, while keeping some features of the hydrodynamic problem. We take a variant of the two-dimensional system used in [14] to introduce some elementary concepts of the theory of dynamical systems. This system of two ordinary differential equations for two variables $\mathbf{X} = (X_1, X_2)$ formally reads $\mathrm{d}\mathbf{X}/\mathrm{d}t = \mathbf{F}(\mathbf{X})$. The vector field $\mathbf{F} = (F_1(X_1, X_2), F_2(X_1, X_2))$ expands as a linear part + quadratic nonlinearities $\mathbf{F}^{(2)}$ that conserve the (classical) energy defined by $\mathcal{E} = \frac{1}{2}\left(X_1^2 + X_2^2\right)$ (*i.e.*, $X_1 F_1^{(2)} + X_2 F_2^{(2)} \equiv 0$). The components of $\mathbf{X}$ are understood as the amplitudes of modes with specific spatial structures. Assuming that this spatial structure has been analyzed in Fourier modes, we retain the idea that the nonlinear coupling between them results from a $k - 2k$ interaction *via* an energy-conserving Burgers-like advection term $v\partial_x v$. Then, assuming that the primitive field v is truncated as $v = X_1 \sin(kx) + X_2 \sin(2kx)$, we simply get $F_1^{(2)} = \frac{1}{2}kX_1X_2$ and $F_2^{(2)} = -\frac{1}{2}kX_1^2$, which indeed fulfill the required energy condition. For the linear part, we consider two real eigenvalues s_1 and s_2 but we do not assume that it is diagonal in X_1 and X_2 as done in [14]. After appropriate rescalings of time and the dependent variables, we thus take:

$$\frac{\mathrm{d}X_1}{\mathrm{d}t} = F_1(X_1, X_2) = s_1 X_1 + X_2 + X_1 X_2 \,, \tag{2}$$

$$\frac{\mathrm{d}X_2}{\mathrm{d}t} = F_2(X_1, X_2) = s_2 X_2 - X_1^2 \,. \tag{3}$$

where s_1 and s_2 are functions of the control parameter (the Reynolds number in our hydrodynamical context). The state $X_1 = X_2 = 0$ is the basic state of interest and we can assume that it remains linearly stable for all values of the control parameter (s_1 and s_2 always negative), which would correspond to the plane Couette flow or Poiseuille pipe flow case, or that it can become unstable with respect to one mode (*e.g.*, s_1 may become positive while s_2 remains negative), which would be appropriate for the plane Poiseuille flow.

Similar phenomenological models have been introduced previously with the same purpose of testing ideas about the subcritical transition to turbulence. For example, the model introduced by Trefethen *et al.* [16] differs from ours only by the nonlinear term which is also quadratic but is centro-symmetric and non-analytical, and by some specific assumption about the behavior of the eigenvalues with the control parameter. Its natural extension to three dimensions [18] was severely criticized in [17] by Waleffe who considered some modifications able to account for the feedback of the perturbation on the mean flow [19]. Though our model suffers from the same deficiency as those in [16,18] we keep it since our aim is not to fit with the hydrodynamic reality but rather to discuss some non-trivial features associated with subcriticality in simple terms. The model proposed by Gebhardt and Grossmann [20] living in a four-dimensional phase space is more complicated. Its interest lies in the fact that. like for the three-dimensional model in [18], parameter sets can easily be found for which the basic state is in competition with a chaotic regime. A simpler model provides a better insight of the dominant effects which we

feel are captured in (2–3). For example, one can check (i) that orbits never escape to infinity provided that the second mode is stable ($s_2 < 0$) and (ii) that attractors are always fixed points, which makes the analysis particularly easy. The first result derives from a mere change of variable $\{X_i = Y_i + a_i;\ i = 1, 2\}$. Indeed, the Y-energy $\frac{1}{2}(Y_1^2 + Y_2^2)$ always decays initially provided that it is sufficiently large and $s_1 + a_2 < 0$ (even if $s_1 > 0$, *i.e.*, when the first mode is unstable) and $(1 - a_1)^2 - 4|s_2|\,|s_1 + a_2| < 0$, so that a sufficiently large disc centered at (a_1, a_2) is an "absorbing zone." As to the second property, one easily sees that periodic behavior is excluded because, according to Bendixon criterion, a limit cycle cannot exist in a phase-space region where the divergence of the vector flow keeps a constant sign. As a matter of fact, we have $\mathrm{div}\ \mathbf{F} = \partial_{X_1} F_1 + \partial_{X_2} F_2 = X_2 + (s_1 + s_2)$ and, all along the line $X_2 = -(s_1 + s_2)$, the vector field $\mathbf{F}$ is directed towards the half-space $X_2 < -(s_1 + s_2)$ so that all trajectories end in this domain where $\mathrm{div}\ \mathbf{F} < 0$.

The phase portrait of system (2–3) is then determined from its fixed points and the position of invariant manifolds attached to them. The fixed points are the roots of

$$0 = s_1 X_1 + X_2 + X_1 X_2\,, \tag{4}$$

$$0 = s_2 X_2 - X_1^2\,. \tag{5}$$

Inserting the solution of (5), $X_2 = X_1^2/s_2$, into (4) we get:

$$X_1 \left(X_1^2 + X_1 + s_1 s_2\right) = 0\,, \tag{6}$$

which yields either one or three fixed points depending on the value of $s_1 s_2$. The actual control parameter in the problem is therefore $\Delta = 1 - 4 s_1 s_2$. We have one fixed point $\mathrm{O} = (0, 0)$ when $\Delta < 0$ and three fixed points $\mathrm{O} = (0, 0)$, and $\mathrm{M}^{(\pm)}$ with coordinates $\left(X_1^{(\pm)}, X_2^{(\pm)}\right)$ when $\Delta > 0$. The coordinates of the nontrivial fixed points are given explicitly by

$$X_1^{(\pm)} = \frac{1}{2}\left(-1 \pm \sqrt{\Delta}\right)\,, \quad X_2^{(\pm)} = \frac{1}{s_2}\left(X_1^{(\pm)}\right)^2 \tag{7}$$

They emerge "from nothing" at *finite* distance from the basic state for $\Delta = 0$ where they are marginally degenerated (saddle node bifurcation). Figure 3 displays the X_1 coordinate of the fixed points as a function of Δ, solid (dashed) lines indicating linearly stable (unstable) solutions as discussed below.

The origin O corresponds to the basic state. It is always a fixed point and, provided that $\Delta < 0$ it is the only one. Its local stability properties directly derive from (2–3) after dropping the nonlinear terms. Eigenvalues are obviously s_1 and s_2, which shows that O is stable as provided that they are both negative. The linear stability study of the non-trivial fixed points is straightforward and needs not be discussed in detail. Let us just mention that for $\Delta > 0$, their local stability is determined from the roots of the eigenvalue equation:

$$s^2 - s_2^{-1} s \left[s_2^2 + \frac{1}{2}\left(1 \mp \sqrt{\Delta}\right)\right] + \frac{1}{2}\sqrt{\Delta}\left(\sqrt{\Delta} \mp 1\right) = 0\,. \tag{8}$$

In the most interesting range $0 \leq \Delta < 1$, the sum of the roots is negative while their product is negative for solution "$+$" and positive for solution "$-$" Solution "$+$" is therefore always a saddle with two real eigenvalues of opposite sign, whereas solution "$-$" is stable but can be a node or a focus depending on the sign of the discriminant of (8).

The next step is the determination of invariant manifolds that extrapolate the eigendirections at the different fixed points. We shall return to this problem here and there but, for the

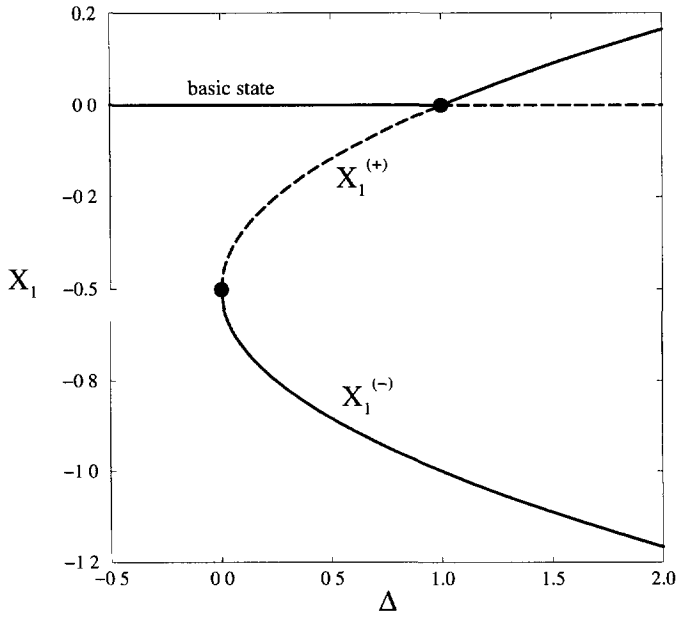


Fig. 3. — Bifurcation diagram of the model: the saddle-node bifurcation takes place at $\Delta = 0$. The basic state experiences a transcritical bifurcation at $\Delta = 1$, where it exchanges its stability with the formerly-unstable nontrivial fixed point.

moment we show the numerically-determined phase portrait of our system in the different cases of interest in Figure 4.

Subfigure 4a corresponds to $\Delta = -0.2 < 0$ (with $s_1 = -0.3$, $s_2 = -1$), so that the origin is the only fixed point. In all the other cases the system has three (marginally two) fixed points but, as seen in subfigures 4b, 4c, and even 4d, the global aspect of the phase portrait in subfigure 4a is preserved. The most striking feature to be observed is the piling-up of trajectories along a "slow manifold" that does not vary much in the vicinity of the bifurcation point. Further, one has to approach the origin in order to discover the differences, as understood from the close-ups in Figure 5.

Considering more particularly case (c) corresponding to $0 < \Delta < 1$, we see that the attraction basins of the origin O and point $M^{(-)}$ are separated by the stable manifold of point $M^{(+)}$ We can also notice that the unstable manifold of $M^{(+)}$ connects O on one side and $M^{(-)}$ on the other.

In the marginal case, $\Delta = 0$, the non-trivial fixed point $M^{(sn)}$ is degenerated with mixed characteristics (saddle-node, hence the notation). From the phase portrait given in subfigure b one understands that $M^{(sn)}$ attracts trajectories initiated in the outer domain limited by its stable manifold, while those initiated in the inner region reach the origin.

The difference between cases $0 < \Delta < 1$ and $1 < \Delta$ is understood entirely on the basis of an exchange of stability between O and $M^{(+)}$, as seen in subfigure 4d. The origin is now a saddle and the non-trivial fixed point $M^{(+)}$ is a stable node, the attraction basin of which is the region inside the loop drawn by the stable manifold of the origin. In fact $M^{(-)}$ is now a stable focus so that the unstable manifold of the origin now coils up around it, but this is not visible at the scale of the figure owing to the large damping rate of trajectories in that region of phase space (at any rate, this is irrelevant to the issues at stake).

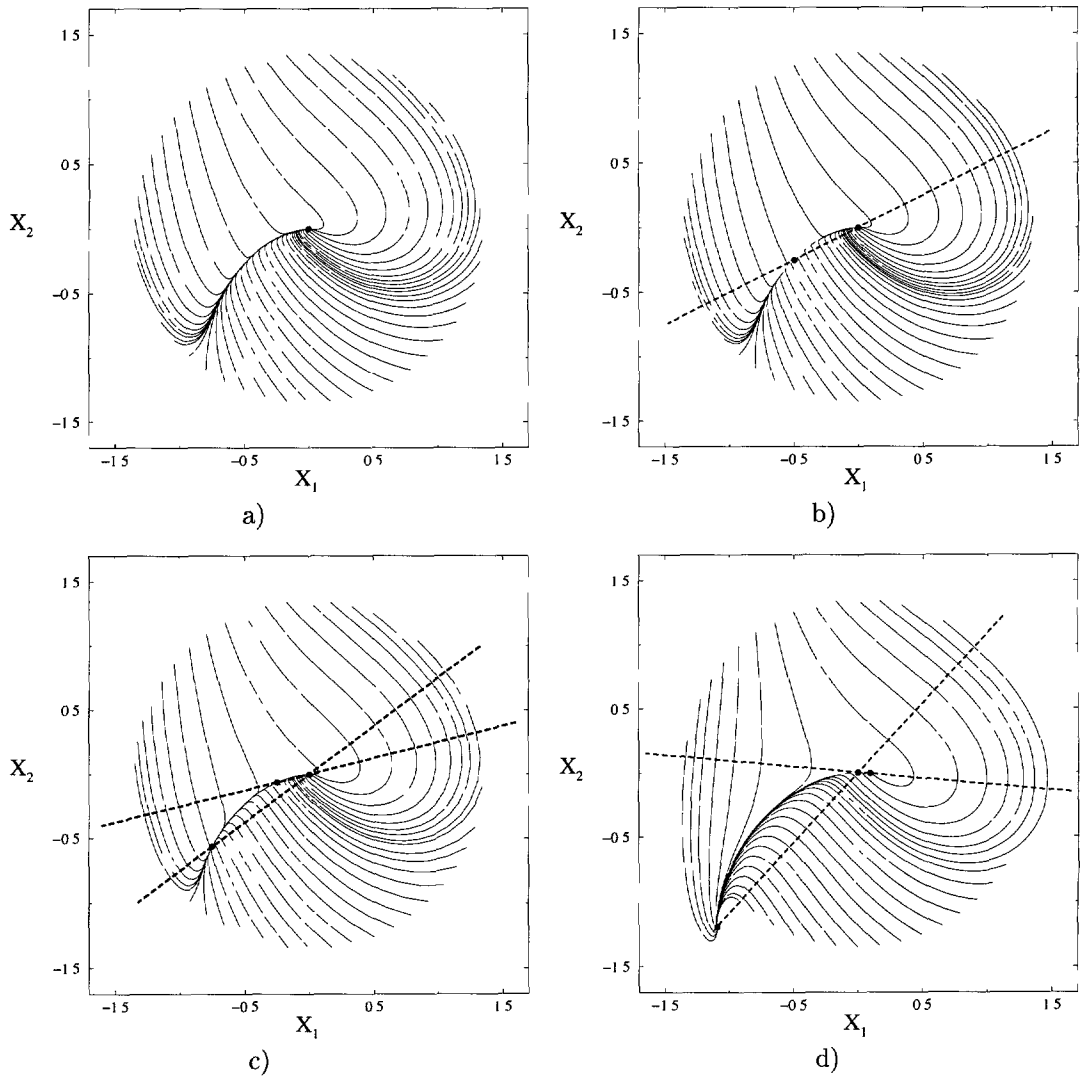


Fig. 4. — Phase portrait of the fully nonlinear problem ($s_2 = -1$): a) $s_1 = -0.30$, $\Delta = -0.20$; b) $s_1 = -0.25$, $\Delta = 0.0$; c) $s_1 = -0.1875$ $\Delta = 0.25$; d) $s_1 = +0.10$, $\Delta = +1.40$. Dashed lines limit the sector where the classical energy is amplified (see § 4).

4. Transient Energy Growth

Let us come back to global stability concepts as applied to the basic state. Studying the evolution of the (classical) energy of a perturbation around the basic state $\mathcal{E} = \frac{1}{2}(X_1^2 + X_2^2)$, we obtain immediately for the full problem the same result as for the linearized problem, *i.e.*,

$$\frac{\mathrm{d}\mathcal{E}}{\mathrm{d}t} = s_1 X_1^2 + X_1 X_2 + s_2 X_2^2 \,, \tag{9}$$

owing to energy conservation by the nonlinear terms. It is readily seen that this quadratic form is definite negative for all initial conditions (X_1, $X_2 = \rho X_1$) provided that the discriminant

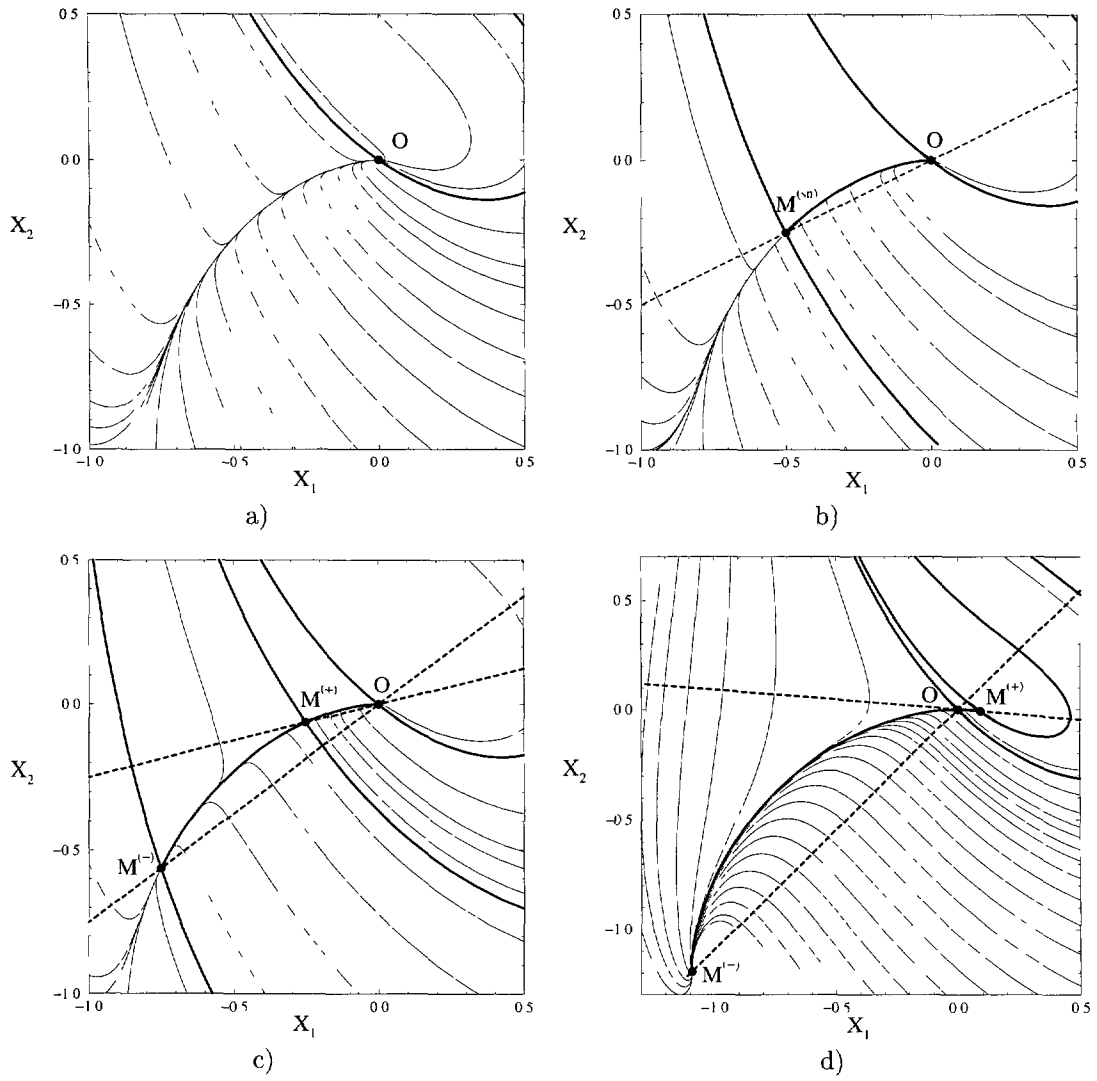


Fig. 5. — Close-up of the nonlinear phase portraits in the vicinity of the origin: a) $\Delta = -0.20$; b) $\Delta = 0.0$; c) $\Delta = 0.25$; d) $\Delta = 1.40$. Stable and unstable manifolds of the different fixed points are indicated by thick lines.

of $s_1 + \rho + s_2\rho^2$ is negative, which yields again $\Delta < 0$. As long as this condition is fulfilled, the basic state is monotonously stable, otherwise there is a sector in phase space defined by $\rho^{(-)} < \rho < \rho^{(+)}$ with

$$\rho^{(\pm)} = \left(1 \mp \sqrt{\Delta}\right) / 2|s_2| \tag{10}$$

where the energy increases. A slightly misleading feature of our model is that the loss of monotonous stability occurs at the same time as the birth of the pair of nontrivial fixed points and hence the loss of global stability. This can be shown to be specific of two-dimensional models with nonlinearities preserving the energy, for which the condition that $d\mathcal{E}/dt = 0$ has non-trivial solutions implies that the system has non-trivial fixed points (the reciprocal

is obvious). However this is no longer general in higher dimensions, as one can understand from the consideration of the celebrated Lorenz model [21]. Indeed, for this well-known three-dimensional system the origin is not monotonously stable while it remains the only fixed point for $r < 1$, and bifurcates supercritically at $r = 1$ ([5]).

The reason for energy growth is easily traced back when considering the phase portrait of the linear stability operator at the origin since $\mathcal{E}$ is just half the squared length of the vector **OM** where M represents the state in phase space at a given time. Trajectories can be guessed from the orientation of the eigenvectors. For eigenvalue s_1 we can choose $X_1^{(1)} = 1$ and $X_2^{(1)} = 0$, and for eigenvalue s_2, $X_1^{(2)} = -u$ with $u = 1/(s_1 - s_2)$ and $X_2^{(2)} = 1$. When s_1 and s_2 are both negative and u is sufficiently large, trajectories may give the impression to run away from the origin (energy growth) though contravariant coordinates of the linearized system in the eigenbasis decay exponentially. This is due to the fact that the eigenvectors are not orthogonal with respect to the canonical scalar product $\langle \mathbf{X} | \mathbf{Y} \rangle = X_1 Y_1 + X_2 Y_2$, owing to the non-normality of the linearized operator, as measured by u.

Figure 6 displays the phase portrait of the linearized problem for $\Delta < 0$ (a), $\Delta = 0$ (b), $0 < \Delta < 1$ (c), and $1 < \Delta$ (d). Transient energy growth leaves no apparent trace in subfigures 6a–c and we have to wait for the fixed point to become unstable, *i.e.*, $s_1 > 0$, $\Delta > 1$, subfigure 6d, to observe a qualitative change. This is confirmed by constructing an appropriate "exotic" energy that always decays, as it should, in the vicinity of a stable fixed point. Indeed taking

$$\tilde{\mathcal{E}} = \frac{1}{2}\left(\tilde{X}_1^2 + \tilde{X}_2^2\right), \tag{11}$$

with

$$\tilde{X}_1 = X_1 + uX_2\,, \qquad \tilde{X}_2 = X_2\,, \tag{12}$$

one obtains

$$\frac{\mathrm{d}\tilde{\mathcal{E}}}{\mathrm{d}t} = s_1\tilde{X}_1^2 + s_2\tilde{X}_2^2 - u\left[\tilde{X}_1^3 - 2u\tilde{X}_1^2\tilde{X}_2 + (u^2-1)\tilde{X}_1\tilde{X}_2^2 + u\tilde{X}_2^3\right]. \tag{13}$$

Hence $\mathrm{d}\tilde{\mathcal{E}}/\mathrm{d}t$ is negative provided that s_1 and s_2 are negative and $(\tilde{X}_1, \tilde{X}_2)$ are sufficiently small, so that the quadratic terms dominate the cubic ones. This property reflects the *local* stability of the basic state. Transient growth of the classical energy is in fact the trace of secular growth in the case of degenerate eigenvalues, as accounted for by a non-diagonal Jordan canonical form ($u \to \infty$). But even in this case an appropriate always-decaying exotic energy can be defined: for our model, assuming $s_1 = s_2$, the quantity $\tilde{\mathcal{E}} = \frac{1}{2}\left(X_1^2 + \gamma X_2^2\right)$, will display the searched property provided that $\gamma > 1/4s_1^2$. This can be easily extended to higher dimensions and applied, *e.g.*, to the three dimensional model used in [18].

Observable $\mathcal{E}$ thus gives a distorted view of the relaxation of small perturbations, which $\tilde{\mathcal{E}}$ does not, as it encodes the stability properties of the basic state (see Fig. 7).

The real problem is whether or not $\mathcal{E}$ regains some interest for the complete nonlinear problem since, as already mentioned, some ambiguity comes from the fact that in hydrodynamics nonlinearities conserve the "classical" energy contained in the perturbations. We should first

([5]) The Lorenz model reads: $\mathrm{d}X_1/\mathrm{d}t = \sigma(X_2 - X_1)$, $\mathrm{d}X_2/\mathrm{d}t = rX_1 - X_2 - X_1X_3$, and $\mathrm{d}X_3/\mathrm{d}t = X_1X_2 - bX_3$; r is the natural control parameter; σ and b are two parameters usually taken as 10 and 8/3, respectively. The classical energy is governed by $\mathrm{d}\mathcal{E}/\mathrm{d}t = -\sigma X_1^2 + (r+\sigma)X_2X_1 - X_2^2 - bX_3^2$, which is definite negative provided that $\sigma X_1^2 - (r+\sigma)X_2X_1 + X_2^2$ is definite positive, *i.e.*, for $(r+\sigma)^2 < 4\sigma$. This is clearly not the case for $r > 0$ and $\sigma = 10$. So the energy is not monotonously decaying for some initial conditions. In the same time, a fixed point fulfills $X_1 = X_2$ but in that case $\mathrm{d}\mathcal{E}/\mathrm{d}t = -(1-r)X_1^2 - bX_3^2$, which is definite negative for $r < 1$ as expected.

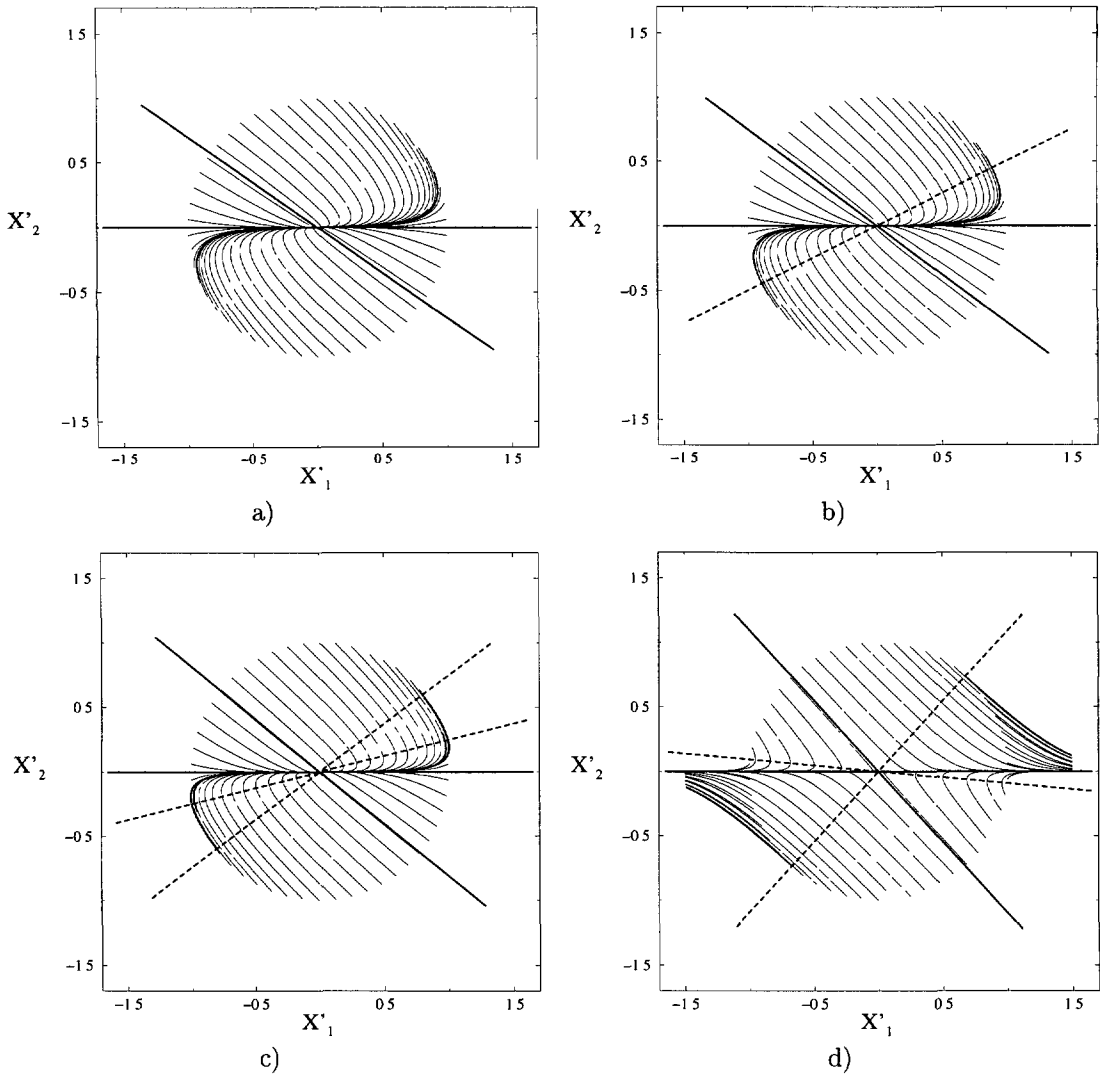


Fig. 6. — Phase portrait of the linearized problem for $s_2 = -1.0$: a) $s_1 = -0.30$, $\Delta = -0.20$; b) $s_1 = -0.25$, $\Delta = 0.0$; c) $s_1 = -0.1875$, $\Delta = +0.20$; d) $s_1 = +0.10$, $\Delta = +1.40$. Here we denote the coordinates as X_1' and X_2' instead of X_1 and X_2 to stress the fact that they are infinitesimal perturbations living in the tangent plane. Eigendirections are marked by thicker lines. The sectors where the classical energy is amplified, given by condition (10), are indicated by dashed lines. They just open at $\Delta = 0$ and widen as Δ increases up to encompass the X_1 direction when $\Delta > 1$.

insist on the fact that considerations about transient energy growth derived from the analysis of the linearized problem are mostly misleading from a *conceptual* point of view. In the study of complicated realistic problems, technicalities obscure the fact that, in a *temporal* setting, all modes are damped in the absence of eigenvalues with positive real part (as further evidenced by using the appropriate "exotic" energy). But one should not attribute any special role to initial states with maximum initial energy growth or at the origin of trajectories with maximum overall energy growth. In our simplistic model such states have obvious geometrical

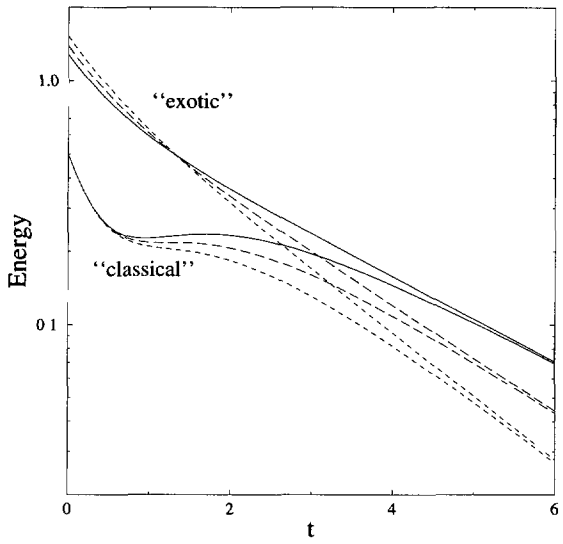


Fig. 7. — a) Evolution of the "classical" and "exotic" energies $\mathcal{E}$ and $\tilde{\mathcal{E}}$ as a function of time for infinitesimal perturbations and $\Delta = 0.20$ (dashed line), $\Delta = 0.36$ (long dashed), and $\Delta = 0.9$ (solid line).

interpretations: as already pointed out, condition $d\mathcal{E}/dt = 0$ in (9) determines sectors in phase plane limited by rays $\rho = X_2/X_1 = \rho^{(\pm)}$, given by (10), which implies that trajectories enter and leave these sectors orthogonally to the corresponding rays ([6]). Maximum instantaneous amplification of $\mathcal{E}$ occurs along some intermediate ray and "optimal" states belong to the entrance rays, the overall amplification being measured by the ratio of the distance at the exit of the sector to the distance at the entrance.

Clearly, even though the amplification ratio may be very large, there is nothing special about these trajectories in a strictly linear context (Figs. 6a–c). This fact has no connection with the amount of energy they contain at the beginning, that is to say the initial distance to the origin, since linearity implies similarity along rays. Furthermore other trajectories may or may not experience analogous transient linear growth depending on the sector in which they start. At any rate, energy growth can take place only at the expense of the basic state, which in general tends to decrease the effective non-normality of the linear stability operator [17] as soon as the energy contained in the perturbation is not infinitesimal in the mathematical sense. Stated in the words of dynamical systems theory, it is not legitimate to extrapolate the tangent dynamics at the origin to the full phase space. Indeed, comparing Figure 4a with the corresponding linear portrait in Figure 6a, we see that nonlinearities already have marked effects, even below the threshold for monotonous stability.

In fact, the idea of optimal states corresponding to "dangerous" initial conditions relates to the nonlinear exploitation of these linear results. However, one can readily solidify this idea in our case by considering the trajectory that starts at the intersection of the stable manifold of the unstable fixed point $M^{(+)}$ and the ray $\rho^{(+)}$ with $X_1 < 0$, see Figure 5c. Trajectories starting along the same ray but with a smaller energy decay to the origin, whereas those with a larger energy go directly to $M^{(-)}$ While it is clear that this state is "optimal" in the desired

([6]) Since $d\mathcal{E}/dt = X_1F_1 + X_2F_2$, condition $d\mathcal{E}/dt = 0$ means that the vector field (F_1, F_2) at point (X_1, X_2) is perpendicular to the rays $X_2/X_1 = \rho^{(\pm)}$

sense, from the comparison between linear and nonlinear phase portraits in Figures 6 and 4, it is also clear that this has little to do with linear properties but much more with the fact that nonlinearities allow for multiple solutions, which in turn puts severe constraints on the dynamics *via* the stable and unstable manifolds attached to them ([7]). It can also be noted in passing that trajectories starting along the ray $\rho^{(+)}$ but with $X_1 > 0$ do not go directly to $M^{(-)}$ but always experience a period of decay when they leave the energy-amplification sector. Their ultimate fate depends also on their initial energy but it cannot be determined so easily since it rests on the precise position of the same manifold but at a "large" distance of its fixed point.

To conclude this discussion, let us remark that the very term of "mode" is not all-purpose but should be reserved to states that preserve themselves in some sense. The special trajectories exhibited above should therefore not be called "modes" by contrast with eigenmodes of the linearized problem that genuinely preserve their shape. In a nonlinear context the term is most appropriately fitted to "states belonging to the slow manifold" of the origin (conspicuous in Fig. 4). Self-preservation would then be accounted for by a *nonlinear* relation that could be obtained by "adiabatic elimination" of fast variables so that the corresponding manifold naturally arrives at the origin along its *least stable* eigendirection (here X_1 with $s_1 < 0$ and $|s_1| < |s_2|$). Such nonlinear modes are therefore *not* special combinations of linear modes governed by the linear operator and cannot be obtained by a linear calculation but the idea gets reinforced that the most slowly relaxing linear modes are of fundamental importance to the transition problem.

5. Implications for Experiments

In this section we attempt to make a connection between the output of simple models such as (2–3) and the nature of the transition to turbulence in globally subcritical hydrodynamical systems such as Couette/Poiseuille flows.

In that our perspective rests on the qualitative theory of dynamical systems, the global (*i.e.*, nonlinear) stability of the basic state thus depends on whether allowed perturbations can be outside its attraction basin, which is therefore the relevant object to explore. This usually amounts to determining the *separatrices*, *i.e.*, the stable manifolds of unstable limit sets, a fully nonlinear problem difficult to grasp empirically from laboratory experiments. In order to clarify this issue, let us make a fundamental distinction between "natural" and "triggered" transition. In the case of a natural transition, uncontrolled perturbations (either due to imperfections of the experimental set-up or to residual turbulence) play the essential role in instability, with statistically reproducible results obtained only at constant noise statistics. By contrast, in the triggered case, artificial perturbations are introduced and, as long as the experimental procedure is not changed, reproducible results can be recorded as a function of the "intensity" of these perturbations. Triggering turbulent spots is a long-standing practice in Poiseuille or boundary layer flows [3, 4]. It has been mastered only more recently in plane Couette flow [6] or Poiseuille pipe flow [7].

No specific perturbations are assumed in case of a natural transition, only their average level. In phase space, supposing that the noise level can be measured by the energy of its perturbations, the corresponding domain is a disk of radius ϵ centered at the origin and the bifurcation has a finite probability to take place as soon as this disk is no longer entirely

([7]) In this respect the best imprint of nonlinearities on the system is the shape of the invariant manifold tangent to the most stable eigendirection at the origin (especially since system (2–3) displays no spurious symmetry obscuring the problem).

contained in the attraction basin of the basic state. Here, the corresponding threshold can be computed from the condition that the disk is tangent to the separatrix at $M^{(+)}$ (the optimal state defined above lies on the disk boundary). The noise in the experimental set-up being measured by ϵ, this threshold is then obtained by solving this condition for Δ. Assuming a specific behavior of Δ as a function of the actual physical control parameter r, one can then determine explicitly how this threshold varies with r. Assuming for example $s_i \sim 1/r$ (see below (14) for a concrete application of such a premise often used in simplified models [16,18,19]), one readily obtains from (7) that the distance between the origin and the stable manifold of $M^{(+)}$ varies as $1/r^3$ in the limit of large r. An examination of Figure 5c indeed shows that, at lowest order in $1/r$, this distance behaves as the length of vector $\mathbf{OM}^{(+)}$ [$\sim 1/r^2$ after (7)] times the tangent of the angle between the X_1-axis and the stable eigendirection at $M^{(+)}$ [$\sim 1/r$ as obtained from a straightforward computation using (8)]. It is interesting to compare this estimate to the sufficient stability condition derived from (13) by finding the maximum $\tilde{\mathcal{E}}$ for which $\mathrm{d}\tilde{\mathcal{E}}/\mathrm{d}t$ remains negative at given (s_1, s_2). Under the same assumptions, cubic terms are easily seen to be of the same order as the quadratic terms for $\tilde{X}_1 \sim 1/r^4$ so that stability of the origin is guaranteed under an asymptotically more stringent condition. This again illustrates the fact that global stability conditions from energy methods are only *sufficient* conditions for stability and generally yield deceptively "conservative" bounds. For the plane Couette flow, the threshold Reynolds number for monotonous stability is $\mathrm{Re_m} \simeq 20.7$ [13] whereas global stability apparently holds up to $\mathrm{Re} \approx 300$ and current best bounds for the perturbation amplitude varies as $\mathrm{Re}^{-21/4}$ at large Re, which is much more severe than what is actually observed, *i.e.*, $\sim \mathrm{Re}^{-1}$ as determined from numerical experiments [22]. Note however that such criteria are of limited relevance since, after all, the subcritical transition to turbulence takes place at large but not asymptotically large values of the Reynolds number in flows such as the plane Couette flow or the Poiseuille pipe flow.

The situation is different for a triggered transition. As a matter of fact, introducing a specific perturbation comes to choosing a special initial condition in phase space. It is only when this initial condition is on the "wrong" side of the separatrix ([8]) that one becomes aware of the fact that the bifurcation has taken place. Now, if we assume that, in the absence of noise, the "intensity" of the perturbation can be varied while keeping its "shape", this amounts to saying that initial conditions can be chosen along a specific continuous path in phase space, with the intensity of the perturbation serving as a curvilinear coordinate along this path. The threshold obtained by performing this particular experiment is then expressed as the condition that the corresponding path intersects the separatrix. By varying r, a specific threshold curve is then obtained. It should first be noted that, since in our model the basin of attraction of the origin extends to infinity in the form of a narrow strip (the narrower, the smaller the eigenvalues), if one were "unlucky" the applied perturbation might never cross the separatrix in some range of r, which would lead one back to a situation where the natural transition may become relevant again. Second and more importantly, one should stress the fact that another experimental perturbation design will presumably yield a different threshold curve (also possibly truncated by natural-transition effects), which explains the dispersion of experimental results found in the literature for the transition to turbulence in the plane Couette flow (see [9] for references). So, a given experimental protocol does not leave one with the freedom to select perturbations optimally fitted to the expected transition.

To illustrate these aspects of a triggered transition using (2–3), we now examine the evolution of the energy of perturbations in parallel with the corresponding phase space trajectories for some well-chosen initial conditions mimicking laboratory experiments. To stick to this point of

([8]) *i.e.*, no longer relaxes towards the trivial fixed point.

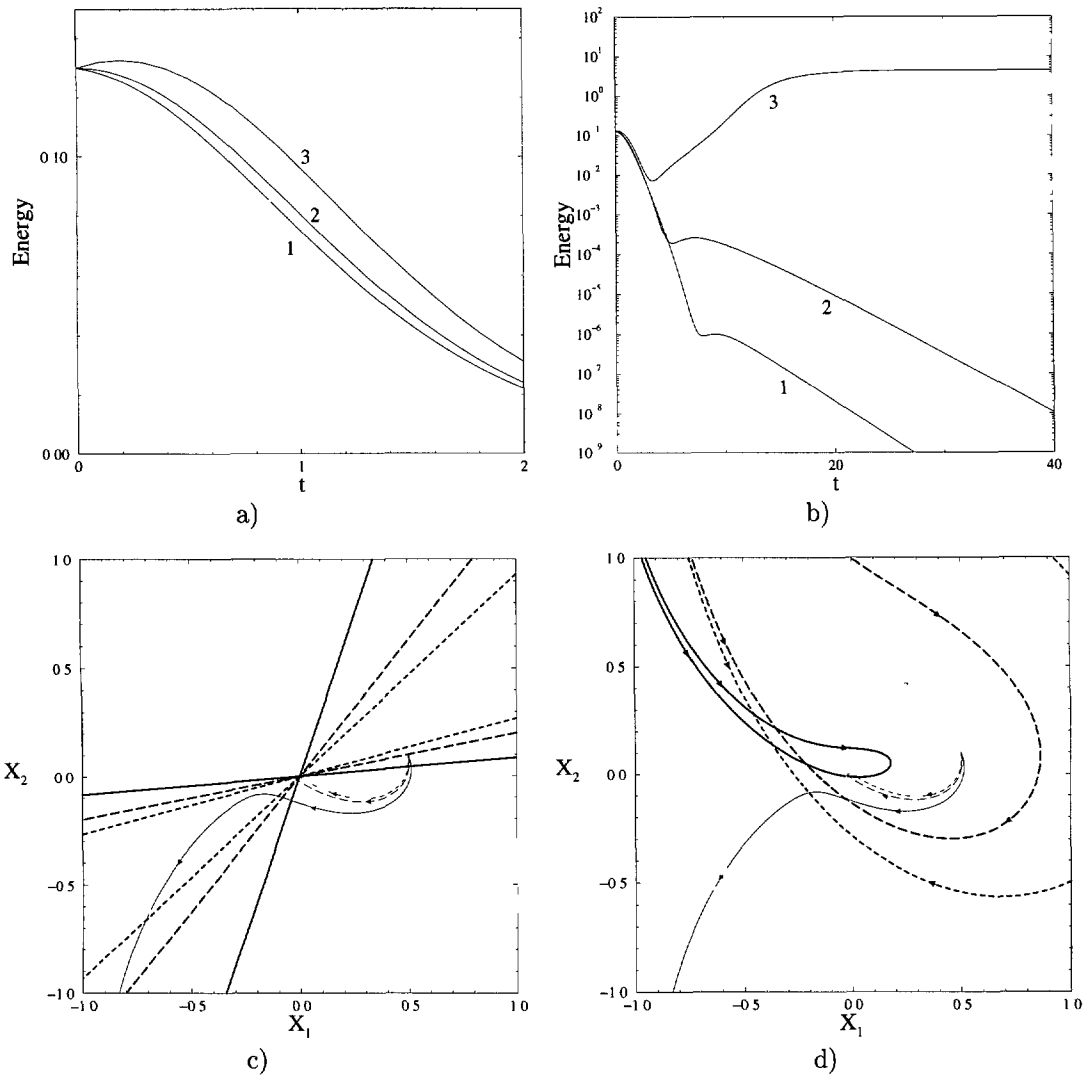


Fig. 8. — a) Initial evolution of the energy for trajectories starting at $X_1 = 0.5$ and $X_2 = 0.1$ for $r = 1.2$ (1), 1.45 (2), 3.0 (3). b) Long term evolution of the energy for the same trajectories. c) Corresponding orbits and sectors of amplified energy: $r = 1.2$ (dashed line), 1.45 (long dashed), 3.0 (solid line). d) Corresponding orbits situated with respect to the separatrices (thick lines following the same conventions).

view, we also assume a specific behavior for the dissipation coefficients s_1 and s_2 as a function of the physical control parameter r, namely,

$$s_1 = -\frac{1}{4r} \quad \text{and} \quad s_2 = -\frac{1}{r}, \tag{14}$$

so that $r_m = r_g = 1$. (By the way, let us recall that by "threshold" we mean "condition for the detection of the global bifurcation" and that, due to a misfortunate feature of our model, the conditions for monotonous and global stability merge together.)

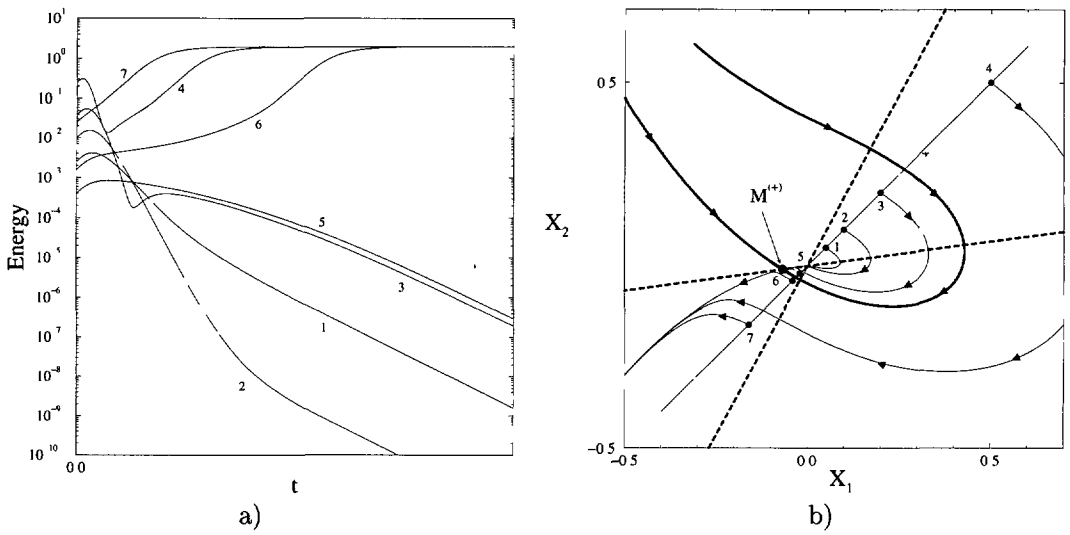


Fig. 9. — a) Evolution of the energy for trajectories with increasing initial perturbation intensity for $r = 2$ and $X_1(0) = X_2(0)$ with $X_1 = +0.05$ (1), $+0.10$ (2), $+0.20$ (3), $+0.5$ (4), -0.02 (5), -0.04 (6), -0.16 (7). b) Corresponding orbits in phase space (the thick line represents the stable manifold at point $M^{(+)}$).

Let us begin with an experiment where the initial perturbation is fixed and the control parameter is varied. As shown in Figure 8a, for trajectories initiated at $X_1 = 0.5$ and $X_2 = 0.1$, initial energy growth manifests itself only when $r > r_1 = 1.45$. Considering now the long term evolution of the energy displayed in Figure 8b, one discovers another critical value $r_2 \simeq 1.848$ below which the energy decays to zero whereas for larger values it reaches some finite value. On the basis of this sole experiment one should however not conclude that $r_m = r_1$ and $r_g = r_2$. This is obvious since as mentioned earlier, all possible perturbations have to be tested for before determining global thresholds, but this is more easily understood when looking at the corresponding orbits in phase space. When varying r, (*i.e.*, Δ) one progressively changes the width of the sector of amplified energy and initial energy growth depends on whether the initial condition is in this sector (Fig. 8c), whereas the final energy level depends on the position of the initial condition with respect to the separatrix at given r (Fig. 8d).

The second kind of experiment at fixed control parameter and variable perturbation intensity can be modeled by a definite relation between the two coordinates of the initial condition. In Figure 9a, we display the behavior of $\mathcal{E}$ for increasing values of $\mathcal{E}$ $(t = 0)$, using $X_2(0) = \rho X_1(0)$ with $\rho^{(-)} < \rho < \rho^{(+)}$, for both $X_{1,2} > 0$ and $X_{1,2} < 0$. Energy growth is always observed at the beginning since we start from appropriate sectors in phase space but, while small perturbations are eventually damped, large enough perturbations may evolve toward the stable nontrivial fixed point. This behavior is at the origin of the misunderstanding expressed in the literature that perturbations experiencing large enough transient growth are able to trigger nonlinear effects and thus lead to a transition. As a matter of fact, the consideration of the corresponding phase portraits (Fig. 9b) clearly indicates that the situation of the initial condition with respect to the separatrix is the only critical issue controlling the long time behavior.

6. Conclusion

In this article, a simplified nonlinear model involving two real variables has been analyzed in detail in order to illustrate some problems arising in the theory of the transition to turbulence in hydrodynamical flows without linearly unstable modes. In such cases, the processes involved are fully nonlinear and the bifurcation can be termed "globally subcritical" to distinguish it from the "locally subcritical" case where the bifurcated state can be obtained by a power series expansion around the basic state. The plane Couette flow and the Poiseuille pipe flow offer classical experimental examples of globally subcritical transitions to turbulence. Our model mimics the hydrodynamical problem in the sense that nonlinearities conserve the energy of perturbations and the linear dynamics is non-normal. This last feature is important since it implies that, even for perturbations that ultimately decay to zero, energy can be observed to grow transiently and that this transient growth is often recognized as a crucial ingredient for the transition to take place. The study is situated in the framework of the theory of dynamical systems. This approach is preferable, since it yields a pictorial interpretation of the transition in terms of phase portraits, fixed points, stable and unstable manifolds, and attraction basins (§ 3). From this model, we find that linear features, and especially transient energy growth, are less important than specifically nonlinear properties, such as the presence of several solutions and the partitioning of the phase space by separatrices. Strikingly, but not surprisingly, the most relevant nonlinear modes appeared to live on a slow manifold emanating from the basic state along the least stable eigendirection and bearing all the interesting stable and unstable steady states.

The key question thus seems to be the determination of other nonlinear solutions when they exist (hence a loss of *global stability*). Unfortunately, for Navier-Stokes equations this is by far not as simple as solving a quadratic equation as with our model! Triggering experiments in the spirit of the "initial value" approach followed here have helped the identification of relevant slowly varying structures involved in turbulent spots, either computationally [5] or experimentally [6]. Such experiments do not however allow one to isolate these structures in order to study their stability. Several strategies have thus been developed to find them by a "continuous deformation" of the primitive problem: for example the plane Couette flow can be reached from the circular Taylor-Couette by decreasing curvature effect progressively [8], from the Couette-Poiseuille plane channel flow by decreasing the applied pressure gradient [9], or by adding a Rayleigh-Bénard convection mechanism of variable strength [10]. Experimentally, the flow profile can also be slightly modified by introducing a wire in the middle plane [23] but the effect of such a forcing may be more difficult to interpret (while leading to an interesting phenomenology [24]) than the addition of an appropriate periodic external perturbation to the Navier-Stokes equations [25]. Of course the continuous deformation approach can be implemented in over-simplified models such as (2–3) by adding a small constant term to (2) and looking for the modified phase portraits but this is not expected to be enlightening, while tackling the hydrodynamical problem at a more realistic level may be more rewarding. Finding nonlinear solutions in different contexts is thus the first step in an analysis of the transition to turbulence parallel to that developed for supercritical flows. The main difficulty comes from the fact that this transition take place at intermediate values of the Reynolds number, *i.e.*, much larger than those sufficient for monotonous stability but not asymptotically large so that viscous effects cannot be neglected.

Finally, the main merit of this work is to provide a better understanding of which issues can and, above all, cannot be extrapolated from a linear framework to a nonlinear one in an easily tractable setting.

References

[1] Landau L.D., *C. R. Acad. Sci. URSS* **44** (1944) 339; reprinted in *Collected Papers of L.D. Landau*, D. Ter Haar, Ed. (Pergamon Press, Oxford, 1965).

[2] Ruelle D. and Takens F., *Comm. Math. Phys.* **20** (1971) 167–192, **23** (1971) 343–344.

[3] Carson D.R., Widnall S.E. and Peeters M.F., *J. Fluid Mech.* **121** (1982) 487–505.

[4] Riley J.J. and Gad-el-Hak M., "The dynamics of turbulent spots", Frontiers in fluid dynamics, S.H. Davis and J.L. Lumley, Eds. (Springer-Verlag, Heidelberg, 1985).

[5] Lundbladh A. and Johansson A.V., *J. Fluid Mech.* **229** (1991) 499–516.

[6] Dauchot O. and Daviaud F., *Phys. Fluids* **7** (1995) 335–343.

[7] Darbyshire A.G. and Mullin T., *J. Fluid Mech.* **289** (1995) 83–114.

[8] Nagata M., *J. Fluid Mech.* **217** (1990) 519–527.

[9] Cherhabili A. and Ehrenstein U., a) *Eur. J. Mech, B/Fluids* **14** (1995) 677–696. b) "Finite amplitude equilibrium states in plane Couette flow", preprint submitted to *J. Fluid Mech.* (1996).

[10] Busse F.H. and Clever R.M., "Bifurcation sequences in problems of thermal convection and of plane Couette flow", Waves and Nonlinear Processes in Hydrodynamics, J. Grue *et al.*, Eds. (Kluwer Academic Publ., 1996).

[11] Morkovin M.V., "The many faces of transition" in Viscous Drag Reduction, Wells, Ed. (Plenum Press, New York, 1969).

[12] see for example: Henningson D.S, Lundbladh A. and Johansson A.V., *J. Fluid Mech* **250** (1993) 169–207.

[13] Joseph D.D., Stability of Fluid Motions, I, Springer Tracts in Natural Philosophy, Vol. 27 (Springer-Verlag, Berlin, 1976).

[14] Manneville P., Dissipative Structures and Weak Turbulence (Academic Press, Boston, 1990).

[15] Henningson D.S. and Reddy S.C., *Phys. Fluid* **6** (1994) 1396–1398.

[16] Trefethen L.N., Trefethen A.E., Reddy S.C. and Driscoll T.A., *Science* **261** (1993) 578–584.

[17] Waleffe F., *Phys. Fluids* **7** (1995) 3060–3066.

[18] Baggett J.S., Driscoll T.A. and Trefethen L.N., *Phys. Fluids* **7** (1995) 833–838.

[19] Waleffe F., *Studies Appl. Math.* **95** (1995) 319–343.

[20] Gebhardt T. and Grossmann S., *Phys. Rev. E* **50** (1994) 3705–3711.

[21] Lorenz E.N., *J. Atm. Sci.* **20** (1963) 130.

[22] Kreiss G., Lundbladh L. and Henningson D.S., *J. Fluid Mech.* **270** (1994) 175–198.

[23] Dauchot O. and Daviaud F., *Phys. Fluids* **7** (1995) 901–903.

[24] Bottin S., Dauchot O. and Daviaud F., "Transition to turbulence in plane Couette flow: the role of streamwise vortices", submitted to *J. Fluid Mech.*

[25] Coughlin K., "Coherent structures and intermittent turbulence in channel flows", submitted to *J. Fluid Mech.*